

Quantum criticality of the sub-ohmic spin-boson model

Stefan Kirchner,^{1,2} Kevin Ingersent,³ and Qimiao Si⁴

¹Max Planck Institute for the Physics of Complex Systems, Nöthnitzer Str. 38, 01187 Dresden, Germany

²Max Planck Institute for Chemical Physics of Solids, 01187 Dresden, Germany

³Department of Physics, University of Florida, P.O. Box 118440, Gainesville, Florida 32611-8440, USA

⁴Department of Physics & Astronomy, Rice University, Houston, Texas 77005, USA

We revisit the critical behavior of the sub-ohmic spin-boson model. Analysis of both the leading and subleading terms in the temperature dependence of the inverse static local spin susceptibility at the quantum critical point, calculated using a numerical renormalization-group method, provides evidence that the quantum critical point is interacting in cases where the quantum-to-classical mapping would predict mean-field behavior. The subleading term is shown to be consistent with an ω/T scaling of the local dynamical susceptibility, as is the leading term. The frequency and temperature dependences of the local spin susceptibility in the strong-coupling (delocalized) regime are also presented. We attribute the violation of the quantum-to-classical mapping to a Berry-phase term in a continuum path-integral representation of the model. This effect connects the behavior discussed here with its counterparts in models with continuous spin symmetry.

PACS numbers: 71.10.Hf, 05.70.Jk, 75.20.Hr, 71.27.+a

I. INTRODUCTION

The standard Kondo model, describing exchange scattering between a local moment and a fermionic band,¹ can be generalized to various Bose-Fermi Kondo models that include coupling of the impurity to one or more bosonic baths. It is conventional to consider bosonic baths described by a power-law density of states

$$\sum_p \delta(\omega - w_p) \propto \omega^{1-\epsilon} \Theta(\omega_c - \omega), \quad (1)$$

where w_p is the dispersion of the bosonic bath (see below), Θ is the Heaviside function, and ω_c is a high-energy cut-off. For a subset of sub-ohmic (positive- ϵ) baths corresponding to $0 < \epsilon < 1$, the Bose-Fermi Kondo problem has a quantum (temperature $T = 0$) phase transition²⁻⁵ between a Kondo phase in which the ground state is a Kondo singlet formed between the local moment and conduction-electron spins, and a local-moment phase in which the coupling to the bosonic bath inhibits the Kondo effect. In all the Bose-Fermi Kondo models that have been studied—corresponding to Ising, XY, and SU(2) symmetry of the bosonic couplings—this transition is continuous.

The Landau theory for continuous phase transitions invokes the fluctuations of an order parameter. For the Bose-Fermi Kondo problem, a suitable order parameter is the local magnetization $M = \langle S^z \rangle$, which vanishes in the Kondo phase but is nonzero throughout the local-moment phase. Within the Landau approach, the quantum criticality is described by a local ϕ^4 theory with a dissipative quadratic term corresponding to a long-ranged interaction in imaginary time: $\frac{1}{2} S^z(\tau) \chi_0^{-1}(\tau - \tau') S^z(\tau')$ with

$$\chi_0^{-1}(\tau - \tau') \sim \frac{1}{|\tau - \tau'|^{2-\epsilon}}. \quad (2)$$

In keeping with the standard theory of quantum criticality, this description is called a quantum-to-classical mapping.

In a study of the Bose-Fermi Kondo model with SU(N) spin symmetry and SU(M) channel symmetry, it was shown in the limit of large N and M with M/N fixed that the quantum critical point (QCP) breaks the quantum-to-classical mapping.⁶ The violation is especially clear for $\frac{1}{2} < \epsilon < 1$. In this range, the local- ϕ^4 description gives rise to a Gaussian fixed point,⁷ and a dangerously irrelevant ϕ^4 coupling leads to a critical static spin susceptibility

$$\chi_{\text{crit}}^{\text{cl}}(T, \omega = 0) \sim \frac{1}{T^x} \quad \text{with } x = \frac{1}{2} \quad \text{for } \frac{1}{2} < \epsilon < 1. \quad (3)$$

However, the large- N results for the local spin susceptibility and Green's function in the quantum critical regime of the SU(N) \times SU(M) Bose-Fermi Kondo model satisfy ω/T scaling, which implies that the QCP is interacting. In particular,

$$\chi_{\text{crit}}^{\text{qu}}(T, \omega = 0) \sim \frac{1}{T^x} \quad \text{with } x = 1 - \epsilon \quad (4)$$

and

$$\chi_{\text{crit}}^{\text{qu}}(T = 0, \omega) \sim \frac{1}{(-i\omega)^y} \quad \text{with } y = x \quad (5)$$

hold over the entire range $0 < \epsilon < 1$. This violation of the quantum-to-classical mapping survives the inclusion of $1/N$ corrections, and has been attributed to the effect of the Berry phase in the spin path-integral representation of the local moment.⁸

Subsequently, a violation of quantum to classical mapping was also discussed for the sub-ohmic spin-boson model.⁹ This model (fully specified in Section II) couples the component S^z of an SU(2) local spin to the displacement of a sub-ohmic bosonic bath with coupling constant

g and the component S^x to a transverse magnetic field Γ . The model has a QCP between a delocalized phase in which the impurity degree of freedom is quenched by the field and a boson-dominated localized phase that retains a two-fold local-moment degree of freedom. These phases are analogous to the Kondo and local-moment phases, respectively, of the Bose-Fermi Kondo model. In the special case where the bosons form an ohmic bath, the spin-boson model and the fermionic Kondo model can be transformed into one another via bosonization¹⁰; however, this transformation breaks down for $\epsilon > 0$. In Ref. 9, it was shown using a bosonic extension^{11,12} of the numerical renormalization-group (NRG) method that the critical exponents for $\frac{1}{2} < \epsilon < 1$ obey hyperscaling (as they do for $0 < \epsilon < \frac{1}{2}$). In particular, just as for the Bose-Fermi Kondo model,^{4,5} the critical local susceptibility satisfies Eqs. (4) and (5), suggestive of an interacting fixed point with ω/T scaling—a conclusion at odds with the quantum-to-classical mapping.

Recently, two sets of Monte-Carlo calculations^{5,13} were carried out for a one-dimensional classical spin chain with long-range Ising interactions $\sum_{i,j} J_{ij} S_i^z S_j^z$, where $J_{ij} \sim 1/|r_i - r_j|^{2-\epsilon}$ for $|r_i - r_j| \gg \tau_0$. Reference 5 applied a cluster Monte-Carlo method at various nonzero values of the short-range cutoff τ_0 , while Ref. 13 used a similar method after taking the limit $\tau_0 \rightarrow 0$. These works both confirmed an earlier conclusion¹⁴ that the critical points of such long-ranged classical spin chains are interacting for $0 < \epsilon < \frac{1}{2}$ and Gaussian for $\frac{1}{2} < \epsilon < 1$, consistent with the predictions of the local ϕ^4 theory.^{7,15}

The results of the classical Monte-Carlo calculations have been interpreted in two very different ways. In Ref. 5, we suggested that these results differ from NRG calculations for the Bose-Fermi Kondo model because a classical spin chain of length L sites does not faithfully represent the quantum-mechanical model at temperature $T = 1/(L\tau_0)$. More specifically, the limit $\tau_0 \rightarrow 0$ of the classical spin chain does not reproduce the path integral of the quantum problem because this limit smears the topological effect of the Kondo spin flips. Along this line, it has recently been shown¹⁶ that a proper path-integral for the sub-ohmic spin-boson model involves a Berry-phase term. Numerically, Ref. 5, generalizing the NRG result of Ref. 4, showed that the temperature dependence of the local spin susceptibility of the Bose-Fermi Kondo model obeys Eq. (4) over about 20 decades in temperature.

By contrast, Ref. 13 assumed the the classical spin chain faithfully represents the spin-boson model. Correspondingly, it interpreted the Monte-Carlo result as demonstrating a fundamental error in the NRG results^{9,11,12} for the sub-ohmic spin-boson model. It was further suggested in Refs. 17 and 18 that over the range $\frac{1}{2} < \epsilon < 1$, the NRG result for the temperature dependence of the local spin susceptibility obeys Eq. (4) due to an artifact of the method, reminiscent of the effect of a temperature-dependent mass term¹⁹ discussed in Ref. 5, and that removal of a spurious $T^{1-\epsilon}$ term from $\chi_{\text{crit}}^{-1}(T)$

exposes an underlying $T^{1/2}$ term representing the true critical behavior.

In this paper, we investigate more thoroughly the temperature and frequency dependences of the local spin susceptibility of the spin-boson model, as calculated using the bosonic NRG approach.^{11,12} The subleading term in the temperature dependence at $\omega = 0$ is shown to be described by an exponent x_2 that depends on ϵ and exceeds $\frac{1}{2}$, contradicting a central assumption of Ref. 18. The exponent y_2 of the subleading term in the frequency dependence at $T = 0$ satisfies $y_2 = x_2$, paralleling the equality $y = x$ of the leading exponents. This provides evidence that both the leading and subleading terms in the local susceptibility satisfy ω/T scaling. Finally, we show that NRG gives consistent frequency and temperature dependences of the local spin susceptibility in the strong-coupling (delocalized) phase. All these features indicate that the temperature and frequency dependences of the critical local spin susceptibility are consistent with an interacting fixed point for $\frac{1}{2} < \epsilon < 1$, thereby augmenting previous evidence for the violation of quantum-to-classical mapping in the sub-ohmic spin-boson and Bose-Fermi Kondo models.

The remainder of the paper is organized as follows. The model and the bosonic NRG method are described in Sec. II. Section III is devoted to the analysis of the leading and subleading terms in the temperature and frequency dependences of the inverse local spin susceptibility at the QCP. In Sec. IV, we discuss the local susceptibility in the strong-coupling (delocalized) phase. Section V addresses the implications of our results, the form of the proper path integral for the spin-boson model, and the role of the Berry phase. The paper concludes with a brief summary in Sec. VI.

II. MODEL AND SOLUTION METHOD

The spin-boson model is described by the Hamiltonian

$$\mathcal{H}_{\text{SB}} = -\Gamma S^x + g S^z \sum_p \left(\phi_p + \phi_p^\dagger \right) + \sum_p w_p \phi_p^\dagger \phi_p, \quad (6)$$

where $S^\alpha = \sigma^\alpha/2$ with σ^α being a Pauli matrix, and ϕ_p annihilates a boson in a bath whose density of states is specified by Eq. (1). The cutoff frequency ω_c entering Eq. (1) will be set to unity and will henceforth serve as the unit of energy.

We have studied the model using the NRG method described in Refs. 11 and 12. The bosonic bath is divided into a set of bins spanning oscillator frequencies $\Lambda^{-(k+1)} < \omega < \Lambda^{-k}$ for $\Lambda > 1$ and $k = 1, 2, 3, \dots$. Within each bin, the continuum of bath states is replaced by a single state, namely, the linear combination of states that couples to the impurity spin. Then the Lanczos method is used to map the spin-boson Hamiltonian to

$H_{\text{SB}}^{\text{NRG}} = \lim_{n \rightarrow \infty} H_n$, where

$$\mathcal{H}_n = -\Gamma S^x + g S^z \sum_p \left(b_0 + b_0^\dagger \right) + \sum_{m=0}^n \left[e_m b_m^\dagger b_m + t_m \left(b_m^\dagger b_{m-1} + \text{H.c.} \right) \right]. \quad (7)$$

As a result of the logarithmic binning, the tight-binding coefficients e_m and t_m that encode the bath density of states decay as Λ^{-m} . This decay allows the Hamiltonian $H_{\text{SB}}^{\text{NRG}}$ to be solved iteratively starting with H_0 and using the eigensolution of H_n to construct the basis of H_{n+1} . The basis of each site of the bosonic chain must be truncated at $b_m^\dagger b_m^\dagger < N_b$. Even with restriction, the dimension of the Fock space grows exponentially with iteration number n . After a few iterations, it is possible to retain only the N_s many-body eigenstates of lowest energy after iteration n . All the results reported below were obtained using $N_b = 24$ and $N_s = 300$.

Our focus in this paper is on the temperature and frequency dependences of the local spin susceptibility. Within the NRG approach, the local static susceptibility is calculated as

$$\chi(T, \omega = 0) = \lim_{h \rightarrow 0} -\frac{\langle S^z \rangle}{h}, \quad (8)$$

where h is a local magnetic field coupling to the S^z component of the localized spin through an additional Hamiltonian term $\Delta H = h S^z$. The imaginary part of the local dynamical susceptibility can be computed as

$$\chi''(T, \omega) = \frac{\pi}{Z_n} \sum_{j,k} |{}_n\langle k | S^z | j \rangle_n|^2 \left(e^{-E_{n,k}/T} - e^{-E_{n,j}/T} \right) \times \delta(\omega - E_{n,k} + E_{n,j}), \quad (9)$$

where $|j\rangle_n$ is a many-body eigenstate of iteration n with energy $E_{n,j}$, and $Z_n = \sum_j e^{-E_{n,j}/T}$. In order to minimize known artifacts of the NRG discretization, we calculate the local susceptibility only at iterations of the same parity (either n even or n odd) and at only one temperature or frequency per iteration: $T_n, \omega_n \propto \Lambda^{-n}$.

III. LOCAL CORRELATION FUNCTIONS AT THE QUANTUM CRITICAL POINT

The QCP is located in our NRG calculations by fixing the transverse field Γ and tuning g . The critical strength g_c is identified as the value of g at which the scaled NRG many-body energies $\Lambda^n E_n$ are independent of the iteration number n , signifying that the system is at a scale-invariant fixed point. This invariance is illustrated in Fig. 1 for two values of ϵ . The critical many-body spectrum is qualitatively similar for all baths corresponding to $0 < \epsilon < 1$.

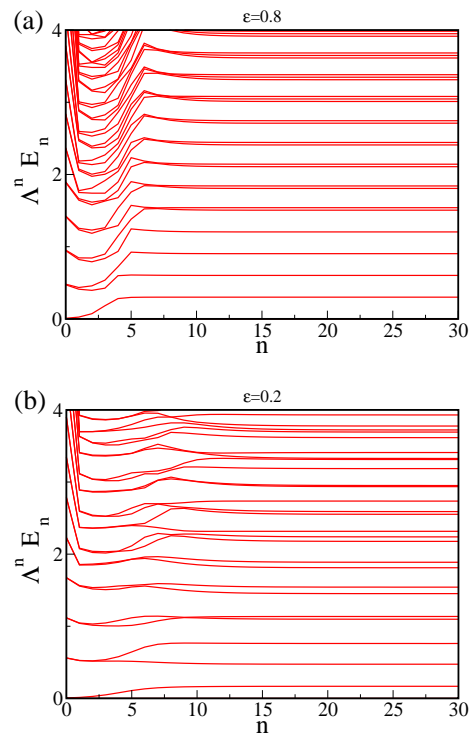


FIG. 1: (Color online) NRG spectra of the spin-boson model at its QCP: Scaled NRG energy $\Lambda^n E_n$ vs iteration number n for a transverse field $\Gamma = 0.01$, NRG discretization $\Lambda = 3$, and bath exponent (a) $\epsilon = 0.8$, (b) $\epsilon = 0.2$. The flatness in the n -dependence of the scaled energy shows that the system is at a renormalization-group fixed point; here, it corresponds to the QCP at $g = g_c$.

A. Temperature dependence of the critical local susceptibility

At the QCP, $g = g_c$, the local static spin susceptibility has a singular temperature dependence. Figure 2(a) is a log-log plot of χ^{-1} vs T for $\epsilon = 0.8$. A least-squares fit (dashed line) of the logarithm of χ^{-1} to the logarithm of a simple power law

$$f(T) = aT^x \quad (10)$$

over $10^{-18} < T < 10^{-4}$ yields a critical exponent of $x = 0.202$. Similar behavior is observed in the local static susceptibility for $\epsilon = 0.7$, fitted over $10^{-19} < T < 10^{-4}$ by $x = 0.301$ [Fig. 3(a)]; for $\epsilon = 0.6$, fitted over $10^{-17} < T < 10^{-4}$ by $x = 0.406$ [Fig. 4(a)]; and for $\epsilon = 0.2$, fitted over $10^{-13} < T < 10^{-4}$ by $x = 0.809$ [Fig. 5(a)]. These temperature exponents are consistent with $x = 1 - \epsilon$ to within about 1.5%.

The modest discrepancies between the exponents x extracted from the numerical data and their interacting values $1 - \epsilon$ can be attributed to a combination of fitting uncertainties and errors associated with the NRG method. Any NRG calculation contains discretization errors introduced by working with $\Lambda > 1$, as well as truncation errors arising from retaining only N_s many-body states

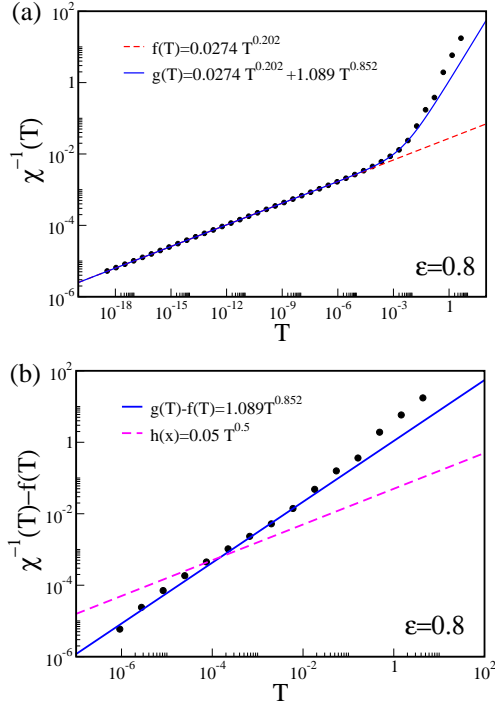


FIG. 2: (Color online) Temperature dependence of the local static susceptibility at the QCP ($g = g_c$). (a) $\chi^{-1}(T)$ for $\epsilon = 0.8$, $\Gamma = 0.01$, and $\Lambda = 3$. The dashed line represents a fit of $\chi^{-1}(T)$ to the leading term $f(T)$ specified in Eq. (10), which yields an exponent $x = 0.202$. The solid line is a fit to Eq. (11) in terms of both leading and subleading terms. (b) Residual $\chi^{-1}(T) - f(T)$ after subtraction of the fitted leading term from (a). The fitted solid line gives a subleading exponent $x_2 = 0.852$. The residual clearly does not have a $T^{1/2}$ dependence (dashed line).

after each iteration. For the bosonic bath treated here, there is also the need to truncate the dimension of the Fock space of each bosonic orbital on the NRG chain to a finite value N_b . One should always bear in mind such sources of systematic error, as one would for any numerical method. Still, several features of the leading-order results serve as nontrivial checks; in particular, the NRG value of the frequency exponent y of the critical local susceptibility (see Sec. III B) agrees with that of an ϵ expansion², and (b) the temperature exponent x and several other critical exponents satisfy hyperscaling relations (as discussed in Sec. V).

Motivated by considerations laid out in the introduction, we further explore the critical behavior by examining the subleading temperature dependence defined through the fitting function

$$\chi^{-1}(T) = aT^x + a_2T^{x_2}. \quad (11)$$

For the case $\epsilon = 0.8$ shown in Fig. 2(a), fitting to Eq. (11) yields a subleading exponent $x_2 = 0.852$. The quality of the fit of the subleading term can be seen more clearly in Fig. 2(b), which plots the residual $\chi^{-1}(T) - f(T)$ after subtraction of the fitted leading term. The residual is

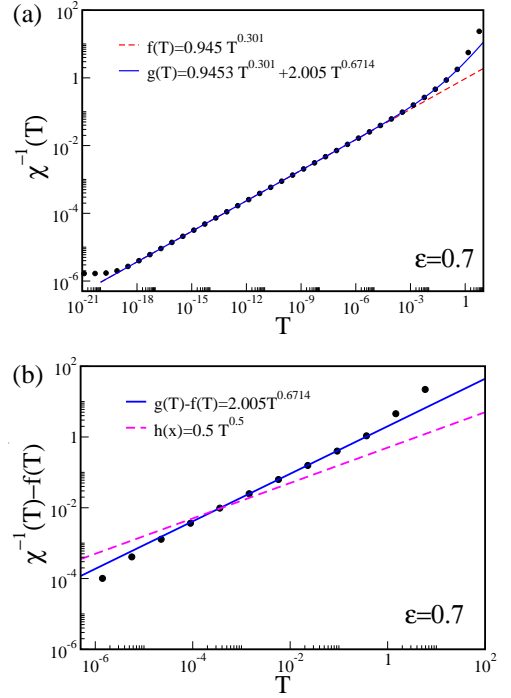


FIG. 3: (Color online) Like Fig. 2 but for $\epsilon = 0.7$, $\Gamma = 1$, and $\Lambda = 4$.

seen to be well-described by a power law over about four decades of temperature $10^{-6} < T < 10^{-2}$. The fitted exponent is different from the value $x_2 = \frac{1}{2}$ that would correspond to the dashed line shown in Fig. 2(b).

Similar results hold for $\epsilon = 0.7$, fitted over $10^{-5} < T < 10^{-1}$ by $x_2 = 0.671$ [Fig. 3(b)]; for $\epsilon = 0.6$, fitted over $10^{-5} < T < 0.5$ by $x_2 = 0.665$ [Fig. 4(b)]; and for $\epsilon = 0.2$, fitted over $5 \times 10^{-5} < T < 0.5$ by $x_2 = 1.25$ [Fig. 5(b)]. For each of the three cases in the range $\frac{1}{2} < \epsilon < 1$ where the validity of the quantum-to-classical mapping is at issue, we find no evidence for the $T^{1/2}$ contribution to $\chi^{-1}(T)$ that is assumed in Ref. 18.

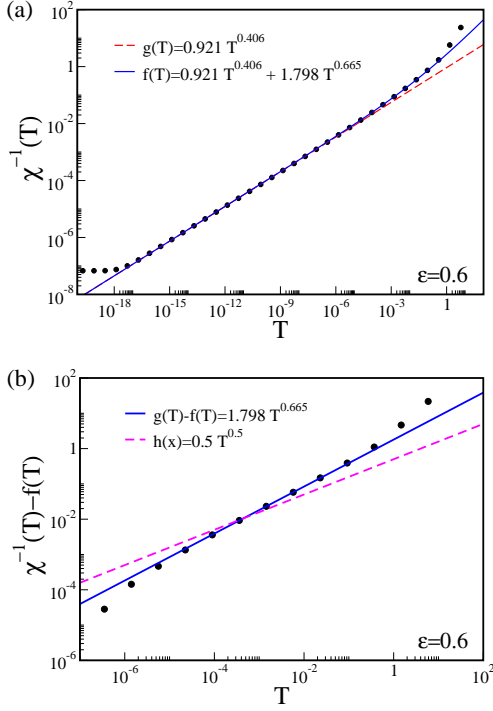
B. Frequency dependence of the critical local susceptibility

Next, we investigate the frequency dependence of the zero-temperature critical local dynamical susceptibility $\chi(\omega)$. Since the NRG delivers $\chi''(\omega) = \text{Im}\chi(\omega)$, this quantity is the focus of our analysis. If necessary, $\chi'(\omega) = \text{Re}\chi(\omega)$ can be obtained via a Hilbert transform of $\chi''(\omega)$, but this procedure introduces some error due to the lower accuracy of the NRG-calculated $\chi''(\omega)$ at high frequencies.

Figure 6(a) plots $\chi''(\omega)$ for $\epsilon = 0.7$. The low-frequency behavior is singular:

$$\chi''(\omega) = \frac{\text{sgn } \omega}{b|\omega|^y}. \quad (12)$$

The exponent is, to an accuracy considerably better than

FIG. 4: (Color online) Like Fig. 3, but for $\epsilon = 0.6$.

1%, $y = 1 - \epsilon = 0.3$. This implies that the full retarded susceptibility has the form specified by Eq. (5). The equality of y and the temperature exponent x is consistent with an ω/T scaling form for the leading scaling term in the inverse local susceptibility.

We will assume that $\chi(\omega)$ has a subleading term with exponent y_2 defined through

$$\frac{1}{\chi(\omega)} = B(-i\omega)^y + B_2(-i\omega)^{y_2}. \quad (13)$$

Correspondingly, for $\omega > 0$,

$$\frac{1}{\chi''(\omega)} \simeq b\omega^y + b_2\omega^{y_2}, \quad (14)$$

where $b = B/\sin(\pi y/2)$,

$$b_2 = B_2 \left[\frac{\cos(\pi(y+y_2)/2)}{\sin(\pi y/2)} + \frac{\sin(\pi y_2/2)}{\sin(\pi y/2)^2} \right], \quad (15)$$

and the approximation in Eq. (14) involves ignoring higher-order terms $\sim \omega^{2y_2-y}$. Fitting to Eq. (14) [Fig. 6(b)] yields an exponent $y_2 = 0.73$ that agrees with the subleading temperature exponent $x_2 = 0.67$ [Fig. 3(d)] to within about 9%. Given that extracting y_2 from $1/\chi''(\omega)$ is less accurate than determining the exponent from $1/\chi(\omega)$ [whose determination requires a calculation of $\chi'(\omega)$, however], we interpret our results as being consistent with $y_2 = x_2$. This suggests that the subleading term of the inverse local spin susceptibility also obeys ω/T scaling.

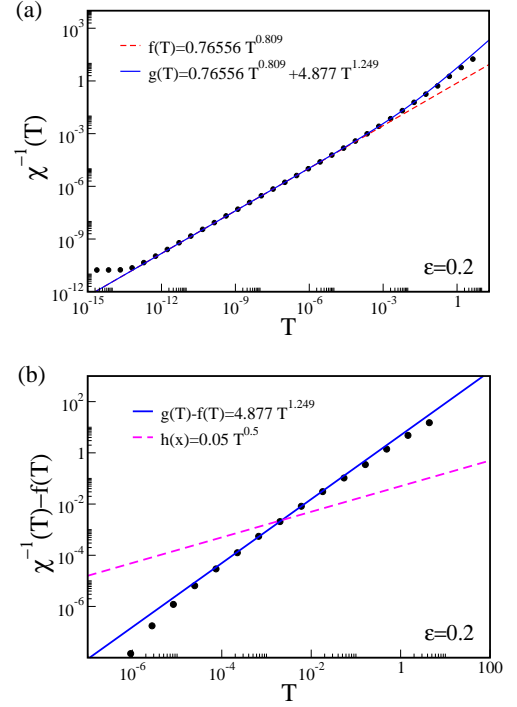
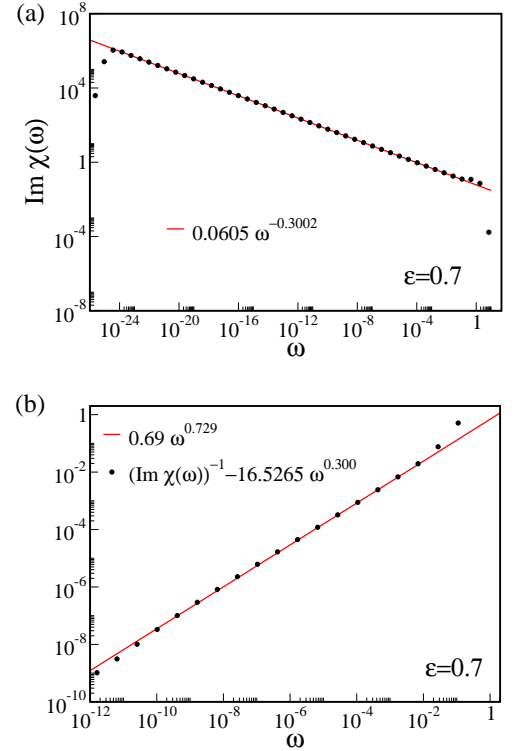
FIG. 5: (Color online) Like Fig. 2, but for $\epsilon = 0.2$.

FIG. 6: (Color online) Frequency dependence of the local dynamical susceptibility at the QCP ($T = 0$, $g = g_c$). (a) $\text{Im}\chi(\omega)$ for $\epsilon = 0.7$, $\Gamma = 1$, and $\Lambda = 4$. The solid line represents a power-law fit to Eq. (12), which yields the exponent $y = 0.3002$. (b) Residual $[\text{Im}\chi(\omega)]^{-1} - b\omega^y$ after subtraction of the leading term inferred from (a). The fitted solid line gives a subleading exponent $y_2 = 0.729$.

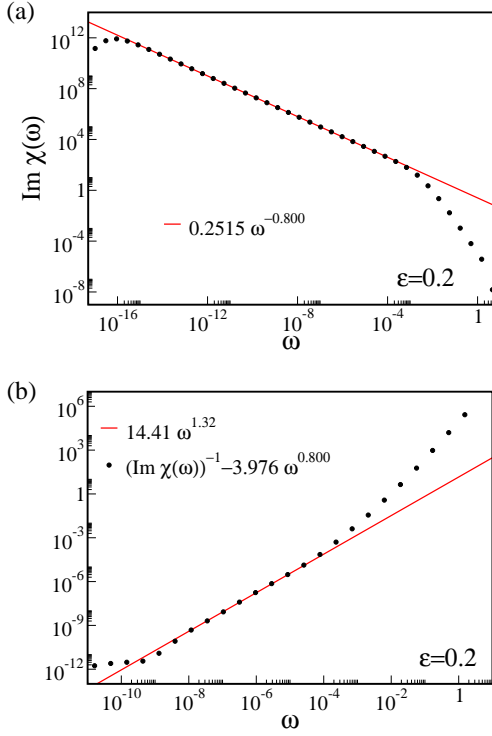


FIG. 7: (Color online) Like Fig. 6, but for $\epsilon = 0.2$, $\Gamma = 0.01$, and $\Lambda = 3$.

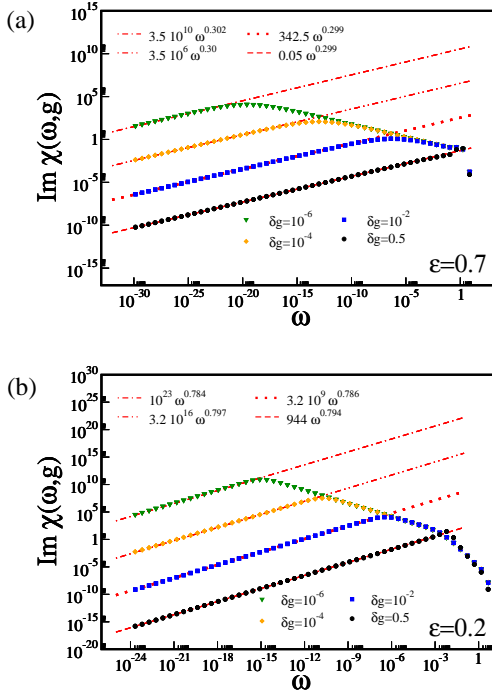


FIG. 8: (Color online) Imaginary part $\text{Im}\chi(\omega)$ of the zero-temperature local dynamical susceptibility at four different bosonic couplings $g < g_c$ or, equivalently, $\delta g \equiv (g_c - g)/g_c > 0$, for (a) $\epsilon = 0.7$, $\Gamma = 1$, and $\Lambda = 4$; and (b) $\epsilon = 0.2$, $\Gamma = 0.01$, and $\Lambda = 3$.

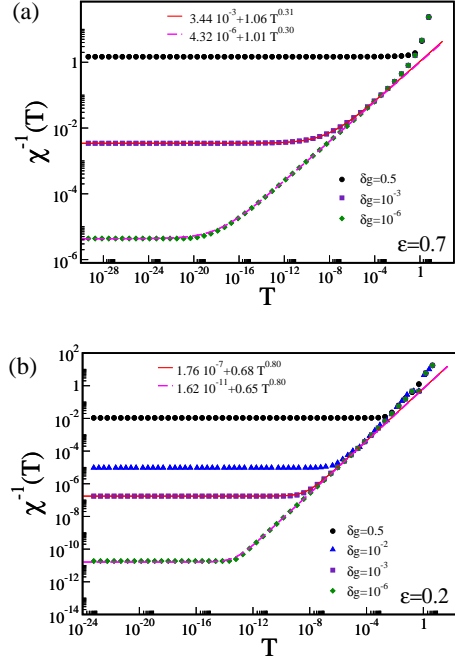


FIG. 9: (Color online) (a) Inverse $\chi^{-1}(T)$ of the local static susceptibility at different bosonic couplings $g < g_c$ or, equivalently, $\delta g \equiv (g_c - g)/g_c > 0$, for (a) $\epsilon = 0.7$, $\Gamma = 1$, and $\Lambda = 4$; and (b) $\epsilon = 0.2$, $\Gamma = 0.01$, and $\Lambda = 3$.

The same procedure can also be applied to the case $\epsilon = 0.2$, as shown in Figs. 7(a) and 7(b). The extracted y is again to a good accuracy equal to $1 - \epsilon = 0.8$, the same as the leading temperature exponent x , so the leading term of the inverse local susceptibility is consistent with ω/T scaling. The fitted value of the subleading frequency exponent is $y_2 = 1.32$, which agrees with the subleading temperature exponent x_2 to within 6%. It is worth noting that for this value of ϵ , which falls in the range $0 < \epsilon < \frac{1}{2}$, the level of agreement between x_2 and y_2 is similar in percentage terms to that for $\epsilon = 0.7$ in the range $\frac{1}{2} < \epsilon < 1$.

IV. LOCAL CORRELATION FUNCTIONS IN THE DELOCALIZED PHASE

To further analyze the NRG results, we turn to the local susceptibility in the delocalized phase, $g < g_c$, which has not received much attention in previous studies. Figure 8(a) shows the ω dependence of $\chi''(\omega)$ at zero temperature for $\epsilon = 0.7$ and several values of $\delta g \equiv (g_c - g)/g_c$. The leading frequency dependence is seen to be $\chi''(\omega) \sim |\omega|^{1-\epsilon}$. The results are well described by

$$\chi(T = 0, \omega, g < g_c) = \frac{1}{A + B(-i\omega)^{1-\epsilon}}. \quad (16)$$

The decrease of $\chi(\omega = 0)$ with increasing δg (i.e., decreasing g) in Fig. 8(a) reflects the increase of A as g

moves away from g_c . These conclusions are also valid for $\epsilon = 0.2$, as seen in Fig. 8(b).

Figure 9(a) shows that for $\epsilon = 0.7$, the local static susceptibility in the delocalized phase is well described by

$$\chi(T, \omega = 0, g < g_c) = \frac{1}{A + aT^{1-\epsilon}}. \quad (17)$$

The same conclusions, once again, apply to $\epsilon = 0.2$, as seen in Fig. 9(b).

We close this section with two general remarks. First, the exponent $1 - \epsilon$ describing the frequency dependence (and, by extension, the temperature dependence), takes the largest possible value that satisfies the Griffiths inequality,²⁰ which states that correlation functions decay in time no faster than does the interaction [as specified in this case by Eqs. (26) and (27) below]. Second, this frequency and temperature dependence only exists in the delocalized phase for $g \neq 0$, implying that turning on the coupling g to the bosonic bath within the delocalized phase is a singular perturbation.

V. DISCUSSION

A. Implications of our results

We have considered in detail the critical behavior of the local spin susceptibility of the sub-ohmic spin-boson model calculated using the NRG. For four different bath exponents spanning the range $0.2 \leq \epsilon \leq 0.8$, we have confirmed that the leading term in the inverse static local spin susceptibility has the $T^{1-\epsilon}$ temperature dependence described by Eq. (4) and demonstrated that the subleading term varies as T^{x_2} with $x_2 > \frac{1}{2}$.

This analysis allows us to assess the alternative interpretations (as outlined in the Introduction) of the Monte-Carlo results for the critical behavior of the local susceptibility in a long-ranged classical Ising chain. In the regime $\frac{1}{2} < \epsilon < 1$, the chain yields a temperature exponent of $\frac{1}{2}$. This originates from a dangerously irrelevant variable, which also leads to a violation of ω/T scaling. In particular, the $T^{\frac{1}{2}}$ dependence of the inverse local susceptibility is not accompanied by a $(-i\omega)^{\frac{1}{2}}$ dependence on frequency. These results differ from those of NRG calculations for the quantum model.

The NRG results presented in Sec. III are consistent with the interpretation advanced in Ref. 5 in the context of the Bose-Fermi Kondo model, namely the difference of the Monte-Carlo results from the NRG results and reflects a violation of the quantum-to-classical mapping. The latter is the result of a Berry-phase term, which we discuss in the next subsection.

Our results are inconsistent with the interpretation put forward in Refs. 13, 17 and 18, which advocates the validity of quantum-to-classical mapping. In this picture, the intrinsic temperature dependence of the inverse critical local susceptibility of the NRG calculation should be

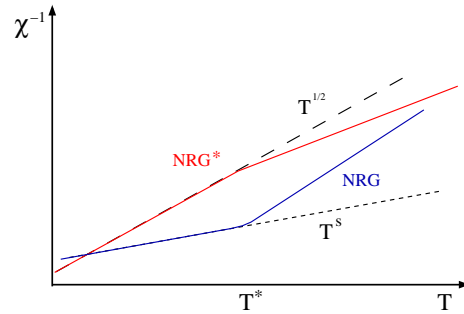


FIG. 10: Schematic log-log plot of the inverse static local susceptibility χ^{-1} vs temperature as obtained using the NRG (cf. Figs. 2–5 of the present paper) and NRG* [cf. Figs. 7(b) and 8(b) of Ref. 18] procedures. The curvature of the NRG* line suggests that a $T^{1/2}$ dependence at $T < T^*$ crosses over at $T > T^*$ to a T^z dependence with a z smaller than $\frac{1}{2}$; this in turn suggests that the asymptotic low-temperature behavior has a temperature exponent less than $\frac{1}{2}$.

$T^{\frac{1}{2}}$, which is masked by an artificial leading $T^{1-\epsilon}$ term. We have shown here that there is no subleading $T^{\frac{1}{2}}$ term in the NRG results.

Reference 18 suggested the possibility of removing the leading $T^{1-\epsilon}$ term using an “NRG*” procedure involving NRG calculations for the spin-boson model supplemented by an *ad hoc* Hamiltonian term containing a coefficient that was adjusted until the inverse local susceptibility at the QCP had a temperature exponent close to $\frac{1}{2}$. Figure 10 provides a schematic comparison between the temperature dependences of the critical static local susceptibilities produced by the NRG (our data from Sec. III A above) and by the NRG* procedure (Figs. 7 and 8 of Ref. 18). If the leading term in $\chi^{-1}(T)$ corresponded to $x = \frac{1}{2}$, then corrections arising from any subleading term with an exponent $z > \frac{1}{2}$ would induce a crossover in $\chi^{-1}(T)$ around some T^* to a higher-temperature behavior with a *greater* slope. Instead, the $\epsilon = 0.6$ and 0.7 NRG* results of Ref. 18 appear to show a T^z dependence with $z < \frac{1}{2}$ for $T > T^*$. One should expect, based on criticality, any such T^z term to persist to sufficiently low temperatures that it, not the $T^{\frac{1}{2}}$ term, dominates the asymptotic behavior.

The T^{x_2} subleading term in the temperature dependence of the critical inverse static susceptibility is accompanied by a subleading term in the frequency dependence of the inverse dynamical susceptibility of the form $(-i\omega)^{y_2}$. Our results are compatible with $y_2 = x_2$ and, in turn, with ω/T scaling for the subleading term (as well as the leading term, where $y = x$). If one interprets both the T^x and T^{x_2} terms in the temperature dependence as artifacts of NRG, then any intrinsic term must vary with a power of T even greater than x_2 ; since $x_2 > \frac{1}{2}$, such behavior would be inconsistent with the validity of the quantum-to-classical mapping. Instead, the result reinforces the conclusion that the fixed point is interacting and features ω/T scaling.

We now briefly discuss other critical exponents describing the variation of the local magnetization $M = \langle S^z \rangle$, the corresponding susceptibility $\chi = \partial M / \partial h|_{h=0}$, and the (imaginary-time) correlation length ξ_τ in the vicinity of the QCP:

$$M(T=0, h=0, g > g_c) \propto (g - g_c)^\beta, \quad (18)$$

$$M(T=0, h, g = g_c) \propto |h|^{1/\delta}, \quad (19)$$

$$\chi(T=0, g < g_c) \propto (g_c - g)^{-\gamma}, \quad (20)$$

$$\xi_\tau \propto |g - g_c|^{-\nu}. \quad (21)$$

An important conclusion from the NRG treatment of the spin-boson model⁹ (as well as that of the Bose-Fermi Kondo model⁴) is that, together with x and y , these exponents satisfy hyperscaling relations²¹ expected to hold at an interacting QCP. Ref. 18 argued that the NRG results for δ and β are invalid for a reason that is entirely separate from mass-flow error, namely the NRG truncation of the bosonic Hilbert space. (A variational procedure has recently been proposed^{22,23} to circumvent the effects of bosonic truncation.) However, it appears unnatural that two independent sources of errors should conspire to yield results that are consistent with hyperscaling.

B. Path integral and Berry phase

Any proper path integral requires taking the continuum limit in time. The quantum critical properties of the Bose-Fermi Kondo model or the spin-boson model can be described within a proper path integral representation. It was shown in Ref. 8 that the hyperscaling observed in the large- N limit of the $SU(N) \times SU(M)$ Bose-Fermi Kondo model even for $\frac{1}{2} < \epsilon < 1$ can be understood as a consequence of a topological Berry-phase term that characterizes the path integral over $SU(N)$. Thus, the breakdown of the quantum-to-classical mapping is not merely an artifact of the saddle point approximation, and it survives the inclusion of $1/N$ corrections.⁸ The path integral over the group $SU(2)$ also involves a Berry-phase term that spoils the reinterpretation of the resulting complex action in terms of a classical action. In other words, the quantum-to-classical mapping cannot be applied for $N = 2$ and the quantum critical properties have to be obtained directly from the quantum model. A proper path integral on $SU(2)$ is given by the functional integral on the Bloch sphere S^2 , the coset space of $SU(2)$. Every path on S^2 is characterized by a geometric phase independent of the spin Hamiltonian. It therefore is natural to expect similar spin path integral representations for the $SU(2)$ Bose-Fermi Kondo model and for the spin-boson or easy-axis Bose-Fermi Kondo model.

It was observed in Ref. 16 that the construction of a Feynman path integral for the spin-boson model through a time-slicing procedure encounters difficulties in taking the continuum limit when using the orthonormal eigenfunction basis of S^z . The standard procedure for circumventing this issue in the case of pure spin Hamiltonians

is to rewrite the short-time propagator as a transfer matrix in spin space.²⁴ A generalization of this method to the spin-boson model rewrites the matrix element of the infinitesimal (imaginary) time evolution operator as

$$\langle \sigma_i \phi_i | e^{-H\tau_0} | \sigma_{i+1} \phi_{i+1} \rangle = e^{\phi_i^* \phi_{i+1}} \mathbf{P}^{i,i+1}, \quad (22)$$

where $\mathbf{P}^{i,i+1}$ is a matrix in the spin subspace, ϕ is a c-number that labels the bosonic coherent states, $e^{\phi_i^* \phi_{i+1}}$ is related to the bosonic Berry phase, and i indexes the time slices. The matrix elements of $\mathbf{P}^{i,i+1}$ are then expressed as the exponential of some function $F(S_i, S_{i+1})$ with $S_i = \pm 1$.¹⁶

$$\mathbf{P}^{i,i+1} \Big|_{S_i, S_{i+1}} = e^{a+b(S_i+S_{i+1})+cS_i S_{i+1}}, \quad (23)$$

with

$$a = \frac{1}{2} [-\omega\tau_0 \phi_{i+1}^* \phi_i + \ln(\Gamma\tau_0)],$$

$$b = -\frac{1}{2} g\tau_0 (\phi_{i+1}^* + \phi_i),$$

$$c = \frac{1}{2} [-\omega\tau_0 \phi_{i+1}^* \phi_i - \ln(\Gamma\tau_0)].$$

Inserting Eq. (23) into the expression for the partition function

$$\begin{aligned} \mathcal{Z} &= \text{Tr} e^{-\beta H} \\ &= A \prod_{i=0}^M \sum_{\sigma_i=\uparrow,\downarrow} \int d\phi_i^* d\phi_i e^{-\phi_i^* \phi_i} \langle \sigma_M \phi_M | e^{-H\tau_0} | \sigma_0 \phi_0 \rangle \\ &\quad \times \prod_{k=0}^{M-1} \langle \sigma_k \phi_k | e^{-H\tau_0} | \sigma_{k+1} \phi_{k+1} \rangle \end{aligned} \quad (24)$$

(where A is a constant and $\tau_0 = \beta/M$), results in an effective action having the form of the action for a classical spin chain coupled to the ϕ -fields with nearest-neighbor interaction $\frac{1}{2} [-\omega\tau_0 \phi_{i+1}^* \phi_i - \ln(\Gamma\tau_0)]$, which is singular as $\tau_0 \rightarrow 0$. However, the terms coupling the bosons are not singular for $\tau_0 \rightarrow 0$, making it difficult to regularize this limit. Nonetheless, keeping track of both the transverse magnetic field Γ and the coupling g to the bosonic bath is essential given that the competition between these two yields the QCP, and also that turning on g is a singular perturbation (as discussed at the end of Sec. IV). A related way to see this difficulty is that, for $\tau_0 \rightarrow 0$, the Kondo-like energy scale goes to zero and the topological effect encoded in the spin flips is suppressed.⁵

On the other hand, in a spin coherent-state representation of the spin-boson model, the continuum limit following a time-slicing procedure poses no difficulty. It leads to a well-defined path integral representation for the sub-ohmic spin-boson model [Eq. (1)]:¹⁶

$$\mathcal{Z} = \int \mathcal{D}[\vec{n}] \exp[-S_{\text{eff}}/2], \quad (25)$$

where the effective action for the spin degrees of freedom is

$$S_{\text{eff}} = -i\mathcal{A}[\vec{n}] - \int_0^\beta d\tau \Gamma n_x(\tau) + \frac{g^2}{2} \int_0^\beta d\tau \int_0^\beta d\tau' n_z(\tau) \chi_0^{-1}(\tau - \tau') n_z(\tau'), \quad (26)$$

where⁵

$$\chi_0^{-1}(\tau - \tau') = \int_0^\infty d\omega \omega^{1-\epsilon} \frac{\cosh[\omega(\beta/2 - |\tau - \tau'|)]}{\sinh(\omega\beta/2)}, \quad (27)$$

and \vec{n} defines a point on S^2 ($|\vec{n}(\tau)|^2 = 1$). The effective action of the sub-ohmic spin-boson problem in the continuum limit contains the Berry-phase term $-i\mathcal{A}[\vec{n}]$, where $\mathcal{A}[\vec{n}]$ is equivalent to the area on the sphere S^2 traced out by $\vec{n}(\tau)$ for $0 \leq \tau \leq \beta$ with $\vec{n}(0) = \vec{n}(\beta)$. As discussed previously for models with continuous spin symmetry⁸, the Berry-phase term in the action, being imaginary, can invalidate the mapping of the quantum action to a classical one.

VI. SUMMARY

We have revisited the critical behavior of the sub-ohmic spin-boson problem. An analysis of the subleading term in the temperature dependence of the inverse local spin susceptibility at the quantum critical point as calculated using the numerical renormalization-group (NRG) method has provided evidence that the intrinsic behavior of the critical static spin susceptibility is given by

Eq. 4 with a non-mean-field exponent. More specifically, we have examined the implications of our data for the two interpretations of the difference (for $\frac{1}{2} < \epsilon < 1$) between Monte-Carlo calculations for a classical Ising spin-chain and NRG calculations for the quantum spin-boson model. The leading and subleading temperature dependences of the critical local susceptibility are consistent only with the interpretation that the classical spin-chain model fails to capture the critical behavior of the quantum model and that the criticality is described by an interacting fixed point characterized by ω/T scaling. This conclusion is further supported by the fact that the subleading frequency dependence of the inverse critical dynamical spin susceptibility has (within numerical uncertainty) the same exponent as that for the subleading temperature dependence of the inverse critical static spin susceptibility.

These results provide evidence for the violation of the quantum-to-classical mapping in the sub-ohmic spin-boson model. We have discussed the effect of a Berry-phase term in a continuum path-integral representation for this model. The importance of the Berry-phase term connects the violation of the quantum-to-classical mapping observed here with that seen in models with continuous spin symmetry.

We thank R. Bulla, J. von Delft, M. Glossop, H. Rieger, M. Troyer, M. Vojta, and T. Vojta for useful discussions. This work has been supported by NSF Grants No. DMR-0710540, DMR-1006985, and DMR-1107814, and by Robert A. Welch Foundation Grant No. C-1411.

-
- ¹ A. C. Hewson, *The Kondo Problem to Heavy Fermions* (Cambridge University Press, 1993).
 - ² L. Zhu and Q. Si, Phys. Rev. B **66**, 024426 (2002).
 - ³ G. Zaránd and E. Demler, Phys. Rev. B **66**, 024427 (2002).
 - ⁴ M. Glossop and K. Ingersent, Phys. Rev. B **75**, 104410 (2007).
 - ⁵ S. Kirchner, Q. Si, and K. Ingersent, Phys. Rev. Lett. **102**, 166405 (2009).
 - ⁶ L. Zhu, S. Kirchner, Q. Si, and A. Georges, Phys. Rev. Lett. **93**, 267201 (2004).
 - ⁷ M. E. Fisher, S. Ma, and B. G. Nickel, Phys. Rev. Lett. **29**, 917 (1972).
 - ⁸ S. Kirchner and Q. Si, arXiv:0808.2647 (2008).
 - ⁹ M. Vojta, N. H. Tong, and R. Bulla, Phys. Rev. Lett. **94**, 070604 (2005).
 - ¹⁰ F. Guinea, V. Hakim, and A. Muramatsu, Phys. Rev. B **32**, 4410 (1985).
 - ¹¹ R. Bulla, N. H. Tong, and M. Vojta, Phys. Rev. Lett. **91**, 170601 (2003).
 - ¹² R. Bulla, H. Lee, N. Tong, and M. Vojta, Phys. Rev. B **71**, 045122 (2005).
 - ¹³ A. Winter, H. Rieger, M. Vojta, and R. Bulla,

- Phys. Rev. Lett. **102**, 030601 (2009).
- ¹⁴ E. Luijten and H. W. J. Blöte, Phys. Rev. B. **56**, 8945 (1997).
- ¹⁵ E. Brézin, J. Physique **43**, 15 (1982).
- ¹⁶ S. Kirchner, J. Low Temp. Phys. **161**, 282 (2010).
- ¹⁷ M. Vojta, N. H. Tong, and R. Bulla, Phys. Rev. Lett. **102**, 249904(E) (2009).
- ¹⁸ M. Vojta, R. Bulla, F. Güttge, and F. Anders, Phys. Rev. B **81**, 075122 (2010).
- ¹⁹ The mass term proportional to $T^{1-\epsilon}$ introduced in Ref. 5 for the classical Ising chain of length $\propto 1/T$ is associated with a change of the interaction potential. This change corresponds to a truncation of “winding” terms of the long-ranged interaction around the periodic chain.
- ²⁰ R. Griffiths, J. Math. Phys. **8**, 478 (1970).
- ²¹ K. Ingersent and Q. Si, Phys. Rev. Lett. **89**, 076403 (2002).
- ²² Y.-H. Hou and N.-H. Tong, Eur. Phys. J. B **78**, 127 (2010).
- ²³ C. Guo, A. Weichselbaum, J. von Delft, and M. Vojta (2011), arXiv:1110.6314.
- ²⁴ M. Suzuki, Prog. Theor. Phys. **56**, 1454 (1976).